AJP

ISSN : 0971 - 3093

Vol 27, Nos 9 -12, September-December 2018

ASIAN JOURNAL OF PHYSICS

An International Research Journal

Advisory Editors : W. Kiefer & FTS Yu

Toshimitsu Asakura

ap

ANITA PUBLICATIONS

FF-43, 1st Floor, Mangal Bazar, Laxmi Nagar, Delhi-110 092, India

B O : 2, Pasha Court, Williamsville, New York-14221-1776, USA

ap

Asian Journal of Physics
Vol. 27, Nos 9-12 (2018) 603-610
Available on: www.asianjournalofphysics.in

Photorefractive optical processing in a correlator by two-wave mixing with a beam-propagation analysis

Yukihiro Ishii[1,2] and Takeshi Takahashi[3]

[1]*Department of Applied Physics, Tokyo University of Science, Katsushika, Tokyo 125-8585, Japan*
[2]*Photonics Control Technology Team, RIKEN Center for Advanced Photonics, Wako 351-0198, Japan*
[3]*Department of Electronic and Information Systems Engineering, Polytechnic University, Kodaira, Tokyo 187-0035, Japan*

This article is dedicated to Prof T Asakura

Enhance Fourier-transformed spectra of an object with high-frequency components by a photorefractive $BaTiO_3$ two-wave mixing are imaged on a phase-only filter of a reference object displayed by a liquid-crystal spatial phase modulator. Beam propagation inside a crystal includes to show an actual process in a two-wave mixing process. The experiments with the high-discrimination capability on the correlation performance are shown.

Keywords: Photorefractive optics, Two-wave mixing, Angular spectrum, Holographic correlator,Pattern recognition.

1 Introduction

The use of nonlinearities in a correlator [1,2] has been studied to improve correlation performance. A phase-only filter (POF) produces sharper correlation peak and better discrimination between similar patterns than those of conventional matched spatial filters [3]. Real-time phase-only matched filtering with liquid-crystal spatial light modulators (LC-SLM's) has been carried out [4,5]. Nonlinear matched filtering, in particular, phase-only filtering has been proposed such that both signal spectrum and filter transfer function are passed through a numerical nonlinearity before they are multiplied in the Fourier domain [6,7].

Photorefractive crystals exhibit a certain predictable nonlinear behavior which is exploited for image processing applications [8,9]. The intrinsic nonlinear properties of crystals have been utilized [10] to propose an all-optical nonlinear joint-transform correlator [11,12]. Photorefractive two-wave mixing has been applied to improve the performance of digital holography while enhancing the SNR of holographic amplitude and phase [13].

In this paper, we demonstrate a photorefractive spectrum-enhanced correlator [14] by two-wave mixing setup to improve the discrimination capability in a pattern-recognition correlation system. Two-wave mixing in a 45°-cut $BaTiO_3$ crystal [15,16] is carried out between an object-bearing beam and a pump beam, and is used as a spatial filter to enhance the high-frequency components of an input test object. During the wave propagation in the crystal, the high-frequency components of an input test object are enhanced by two-wave mixing. As a result, the discrimination capability in the correlator is improved. The beam propagation by two-wave mixing inside a crystal is numerically shown by the beam-propagation method. A reference object to be correlated with a test object is recorded in a phase-only filter [3] displayed by a spatial light modulator (SLM). High discriminate correlation results are shown in the pattern-and character recognition experiments by using two types of crystals; 0°-cut and 45°-cut $BaTiO_3$ crystals.

Corresponding author
e-mail: y.ishii@rs.kagu.tus.ac.jp; (Yukihiro Ishii); *Fax/phone: 8142-560-2833*

2 Enhancement of high-frequency spectra in a test object by two-wave mixing

Figure 1 depicts an experimental setup of a Vander-Lugt type correlation system used for recognizing the patterns. Two-wave mixing in a $BaTiO_3$ crystal is carried out between an object-bearing beam and a pump beam. The polarization in both beams is oriented to be parallel to a plane of an incidence. The object is processed in the Fourier domain.

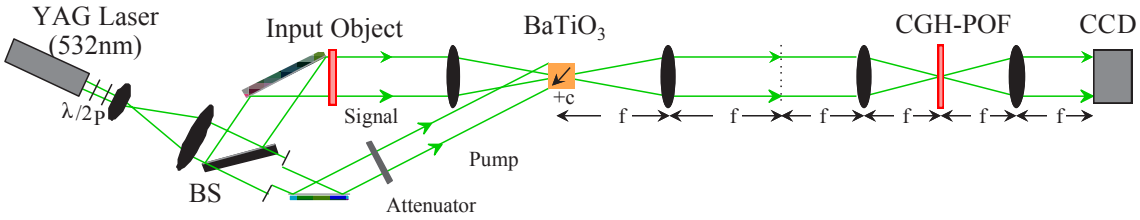

Fig 1. A photorefractive spectrum-enhanced processing by a 0°-cut or a 45°-cut $BaTiO_3$ crystal and a phase-only filter displayed by a spatial-light phase modulator in a correlator.

We model the energy transfer process through a set of coupled-wave equations [17] when the two laser beams enter the photorefractive $BaTiO_3$ crystal from the same side at $z = 0$. A set of coupled-wave equations are written as

$$\frac{dA_s}{dz} = \frac{\Gamma}{2I_0}|A_p|^2 A_s - \frac{\alpha}{2}A_s$$
$$\frac{dA_p}{dz} = -\frac{\Gamma}{2I_0}A_p|A_s|^2 - \frac{\alpha}{2}A_p \tag{1}$$

where A_s and A_p are the amplitudes of the signal and pump beams, respectively, A_s stands for the Fourier spectrum of an input test object, Γ is the coupling coefficient which is considered to be real for the $BaTiO_3$ crystal that dominates the diffusion field, α is the absorption coefficient, I_0 is total input intensity, i.e., $I_0 = |A_s|^2+|A_p|^2$, and z is the longitudinal axis along which the interaction occurs in length l. The spectrum-enhanced amplitude $A_s(\xi,\eta;l)$ of the signal (object) beam by two-wave mixing between signal and pump beams through coupled-wave equations in Eq (1) is given by

$$A_s(\xi,\eta;l) = G(\xi,\eta;0)\sqrt{\frac{(1+|G(\xi,\eta;0)|^2/I_{pc})\exp(\Gamma l)}{1+(|G(\xi,\eta;0)|^2/I_{pc})\exp(\Gamma l)}}, \tag{2}$$

for a negligible absorption ($\alpha \approx 0$), where G is the amplitude of signal beam that is Fourier spectrum of a reference object g, (ξ, η) are the spatial frequency coordinates, and I_{pc} is the intensity of a collimated pump beam at $z=0$, i.e., $I_{pc}=I_p(\xi,\eta;0)=|G(\xi,\eta;0)|^2_{\max}/\beta$. The pump beam intensity is chosen to get the optimum enhancement feature by minimizing a cost function E. The cost function is defined as the standard deviation of the amplitude $|A_s(\xi, \eta)|$;

$$E(\beta) = \sqrt{\frac{1}{S}\int_s (|A_s(\xi,\eta)|/\langle|A_s(\xi,\eta)|\rangle - 1)^2\, d\xi d\eta}, \tag{3}$$

where β depicts the ratio of the maximum intensity of Fourier spectrum G to the intensity of pump beam, i.e., $\beta = |G|^2_{\max}/I_p$, S stands for the integration area in Fourier domain, and $\langle|A_s(\xi, \eta)|\rangle$ denotes the mean value of enhanced Fourier spectrum. For our computation, we used a direct search algorithm with the golden section [18] to minimize the cost function $E(\beta)$ with respect to a beam ratio β. If $E(\beta)$ reaches zero, all spectra can approach to be uniform that can be exhibited a hard-clipping characteristic like a pure phase correlator [19] showing a good performance in discrimination capability. Nevertheless, it cannot keep all enhanced spectra to be flat because of the limited coupling coefficient Γ.

A coupling constant Γ is given approximately by

$$\Gamma \approx \frac{4\pi}{\lambda \cos\theta} n^3 r_{42} E^s \sin\alpha \sin 2\alpha, \tag{4}$$

where r_{42} in $BaTiO_3$ crystals is the dominant electro-optic coefficient, n is the index of refraction of a crystal, 2θ is the inter-beam angle between signal and pump beams, E^s is the saturated space-charge field and the parameter α is the angle between the grating wave vector ***K*** and the *c*-axis of the crystal. The coupling constant Γ depends on the angles of the beams and as well as their polarization states. The crystal orientation is shown in Fig 2 for the 45°-cut $BaTiO_3$ crystal relative to the 0°-cut $BaTiO_3$ crystal. An optimum angle α is reduced to 54.7° to maximize the coupling constant Γ in Eq (4) that approaches to zero by making a differentiation dΓ/dα as a function of α in Eq (4). The direction of the grating vector ***K*** shown in the 45°-cut crystal of Fig 2 can be arranged at an angle close to the angle α (= 54.7°)+π with respect to the c-axis at which maximum gain can be attained.

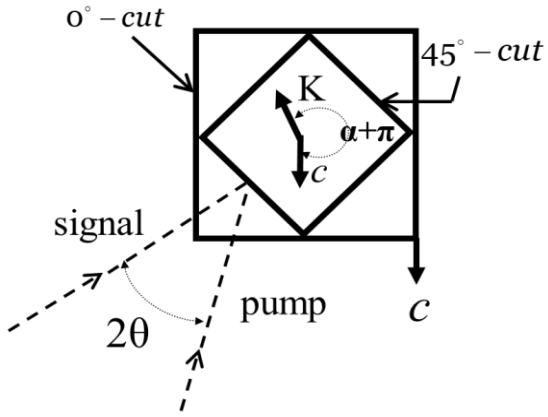

Fig 2. An orientation of the 45°-cut $BaTiO_3$ crystal relative to the 0°-cut $BaTiO_3$ crystal is shown. A c-axis is an optic axis and ***K*** vector is a grating vector. The signal and pump beams interfere each other with an inter-beam angle 2θ. The angle α is optimized by maximizing the coupling constant Γ.

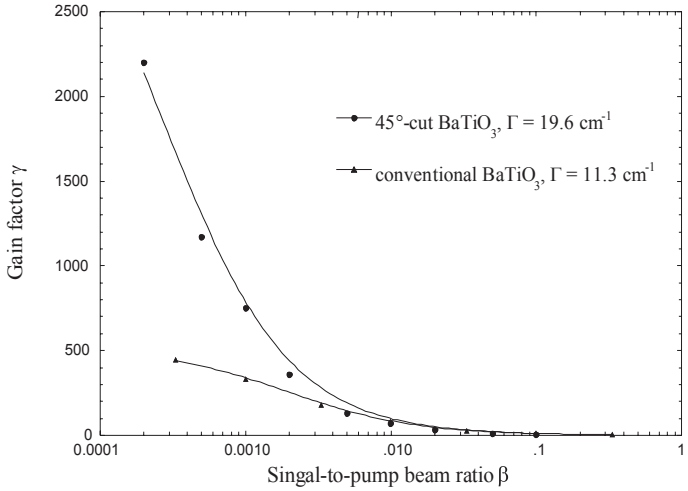

Fig 3. Experimental gain factor γ as a function of a signal-to-beam pump ratio β. The coupling coefficients Γ are obtained by the least-squares estimates.

Figure 3 shows the experimental result of the gain factor γ as a function of a signal-to-beam pump ratio β. The coupling constant Γ is derived from the experimental amplitude gain factor $\gamma = A_s(\xi,\eta; l)/G(\xi,\eta; 0)$ as a function of a signal-to-pump beam ratio β with an inter-beam angle of $2\theta = 30°$. By fitting the experimental data to the amplitude gain factor γ as depicted in Eq (2), the coupling coefficients Γ are obtained as $\Gamma = 19.6\ \text{cm}^{-1}$ showing a large coupling coefficient for $l = 0.42$ cm and $\beta = 5.82$ in a 45°-cut $BaTiO_3$ crystal and $\Gamma = 11.3\ \text{cm}^{-1}$ for $l = 0.55$ cm and $\beta = 7.46$ in a 0°-cut $BaTiO_3$ crystal.

We describe the beam propagation inside a photorefractive crystal by using Fourier analysis. A crystal is oriented to its center $z = z_c$ that is matched to a Fourier-transform plane of an input object $g(x, y)$ such that a Fourier spectrum at a crystal center $z = z_c$ is written as

$$G(\xi,\eta; z_c) = \iint_{-\infty}^{\infty} g(x,y) \exp\left[-j2\pi\left(\frac{x\xi + y\eta}{\lambda f}\right)\right] dxdy \tag{5}$$

By using Eq (5), a Fourier spectrum at a position z inside a crystal is given by

$$G(\xi,\eta; z) = \iint_{-\infty}^{\infty} B\left(\frac{\alpha}{\lambda}, \frac{\beta}{\lambda}; z_c\right) \exp\left[\, jk(z - z_c)\sqrt{1-\alpha^2-\beta^2}\,\right] \exp\left[j2\pi\left(\frac{\alpha}{\lambda}\xi + \frac{\beta}{\lambda}\eta\right)\right] d\left(\frac{\alpha}{\lambda}\right) d\left(\frac{\beta}{\lambda}\right) \tag{6}$$

where $B\left(\frac{\alpha}{\lambda}, \frac{\beta}{\lambda}; z_c\right)$ is an angular spectrum [20] of a Fourier spectrum $G(\xi, \eta; z_c)$ with direction cosines (α, β). Now, a Fourier spectrum $G(\xi, \eta; 0)$ at a front surface of a crystal is an initial amplitude that is inserted into Eq (2). After propagation at Dz, the spectrum-enhanced signal-beam amplitude $A_s(\xi,\eta;\Delta z)$ is given by

$$A_s(\xi,\eta;\Delta z) = G(\xi,\eta;0)\sqrt{\frac{(1 + |G(\xi,\eta;0)|^2/I_p(\xi,\eta;0))\exp(\Gamma\Delta z)}{1 + (|G(\xi,\eta;0)|^2/I_p(\xi,\eta;0))\exp(\Gamma\Delta z)}},$$

Therefore, the spectrum-enhanced signal-beam amplitude $A_s(\xi, \eta; n\Delta z)$ at a n-th step propagation inside a crystal is rewritten as

$$A_s(\xi,\eta;n\Delta z) = A_s(\xi,\eta;(n-1)\Delta z)\sqrt{\frac{(1 + |A_s(\xi,\eta;(n-1)\Delta z)|^2/I_p(\xi,\eta;(n-1)\Delta z))\exp(\Gamma\Delta z)}{1 + (|A_s(\xi,\eta;(n-1)\Delta z)|^2/I_p(\xi,\eta;(n-1)\Delta z))\exp(\Gamma\Delta z)}} \tag{7}$$

for $n \geq 2$, accompanying with a depleted pump-beam intensity $I_p(\xi, \eta; (n-1)\Delta z)$ at a $(n-1)$th step propagation inside a crystal, it is given by.

$$I_p(\xi,\eta;(n-1)\Delta z) = I_p(\xi,\eta;(n-2)\Delta z)\left[\frac{(1 + I_p(\xi,\eta;(n-2)\Delta z)/|A_s(\xi,\eta;(n-2)\Delta z)|^2)\exp(-\Gamma\Delta z)}{1 + (I_p(\xi,\eta;(n-2)\Delta z)/|A_s(\xi,\eta;(n-2)\Delta z)|^2)\exp(-\Gamma\Delta z)}\right] \tag{8}$$

where this equation is held for $n > 2$. For $n = 2$, Eq (8) is reduced to

$$I_p(\xi,\eta;\Delta z) = I_{pc}\left[\frac{(1 + I_{pc}/|G(\xi,\eta;0)|^2\ \exp(-\Gamma\Delta z)}{1 + (I_{pc}/|G(\xi,\eta;0|^2)\exp(-\Gamma\Delta z)}\right]$$

By combining Eq (7) with Eq (8), a numerical simulation of the spectrum-enhanced amplitude $|A_s(\xi,\eta; z)|$ vs. the spectral frequency domain η is demonstrated in Fig 4 that exhibits almost flat response at a rear surface $z = 4.2$ mm of a crystal. Here the signal energy in the high frequencies is enhanced. It thereby helps to improve the discrimination capability to detect the auto- and cross-correlation peaks along a propagation distance z. For the numerical calculation in Fig 4, a Japanese 50-yen stamp was used as the object. Objects used in the correlation test are 50-yen and 80-yen mailing stamps as shown in Fig 5.

The POF located in a CGH-POF plane in Fig 1 has a complex transmittance, i.e.,

$$\frac{G^*(\xi',\eta')}{|G^*(\xi',\eta')|} = \exp\left[-j\phi_G(\xi',\eta')\right] \tag{9}$$

where (ξ', η') are the spatial frequency coordinates at the filter plane and ϕ_G denotes the phase distribution of a reference object in the Fourier domain. The POF is encoded with the technique of a CGH. The correlation output of a target object with a reference object can be represented by the inverse Fourier transform of the products of Eqs (7) and (9). The correlation signals are detected by a CCD camera in Fig 1.

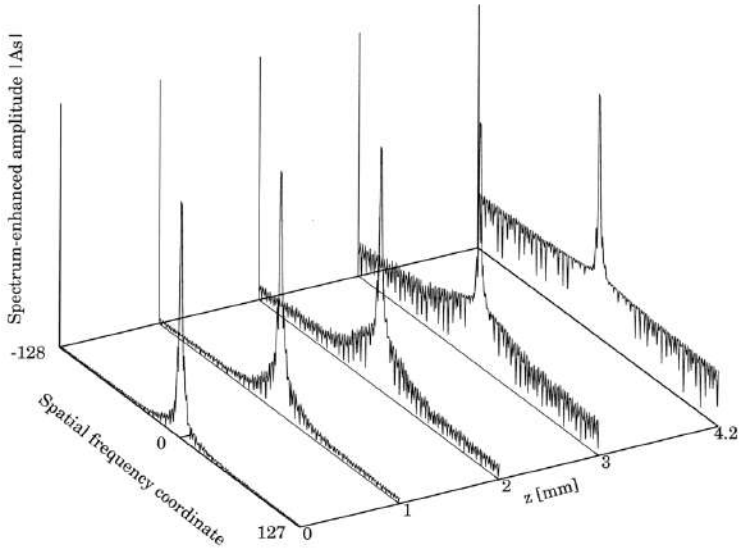

Fig 4. The spectral amplitude $|A_s(z)|$ is calculated by the propagation of the angular spectrum. The enhanced spectrum is shown along a propagation distance z for an input object of a 50-yen stamp. The spectrum amplitude $|A_s(z)|$ at z = 4.2 mm exhibits a flat response in high frequencies, leading to high discrimination capability in the correlation test.

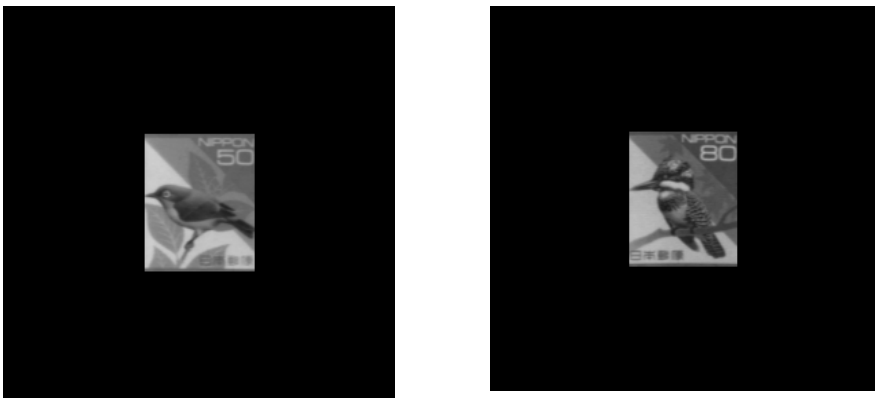

(a) (b)

Fig 5. 50-yen (a) and 80-yen (b) stamp-objects are test objects used in the correlation test for simulations and experiments.

3 Experiments

Experimental setup for the spectrum-enhanced correlator is shown in Fig 1. Two-wave mixing in $BaTiO_3$ crystals is provided by a frequency doubled YAG laser operating at 532 nm with the power of 20 mW. The 0°-cut $BaTiO_3$ crystal has dimensions of a (= 0.47) × b (= 0.55) × c (= 0.52) cm^3, and the 45°-cut

$BaTiO_3$ crystal has dimensions smaller than the 0°-cut crystal. The beam is collimated and is subsequently split by a beam splitter (BS) into signal and pump beams.

Experiments of two-wave mixing in photorefractive $BaTiO_3$ crystals determined the coupling coefficients equal to $\Gamma = 11.3\ cm^{-1}$ and $\Gamma = 19.6\ cm^{-1}$ for the 0°- and 45°-cut $BaTiO_3$ crystals, respectively, as shown in Fig 3. The intersection angle between signal and pump beams has been kept at $2\theta = 30°$ to obtain maximum energy transfer between signal and pump beams. The signal beam carries the object information displayed on an LCD used in a view finder of a digital camera that acts as a spatial-light amplitude modulator. A 20 cm focal-length Fourier-transform lens has been used to obtain the Fourier spectrum of the input object. Fourier spectrum enhanced by two-wave mixing is imaged on to a CGH that is displayed by an LC-SLM that acts almost as a spatial-light phase [5] modulator. The intensity distribution in the correlation output plane is measured by a CCD camera.

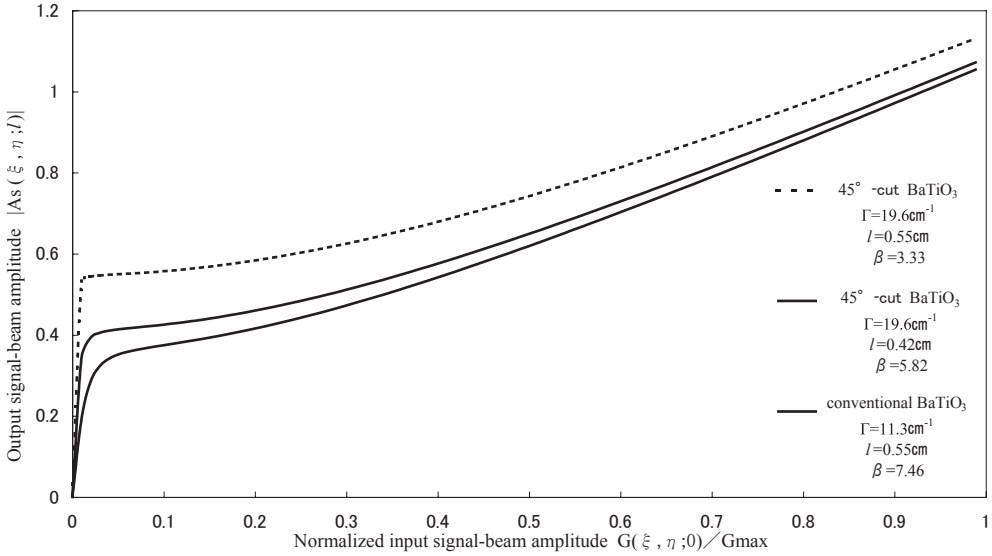

Fig 6. Nonlinear enhancements of signal-beam amplitude as a function of the normalized input signal-beam amplitude for the beam ratios β = 5.82 and β = 7.46 using conventional 0º-cut and 45º-cut $BaTiO_3$ crystals, respectively.

The correlation test is performed for mailing stamps "50-yen" and "80-yen" as shown in Fig 5. A 50-yen mailing stamp is used as a reference object g whose Fourier spectrum is G in Eqs (2) and (9).

Figure 6 shows the nonlinear enhancements of the signal-beam amplitude as a function of the input signal-beam amplitude normalized by its maximum for two interaction lengths in the 45º-cut crystal and an interaction length in the 0º-cut crystal. The optimized beam ratios of β = 7.46 in the 0º-cut crystal and β = 5.82 in the 45º-cut crystal are values when the cost functions $E(\beta)$ in Eq (3) are minimized as $E = 0.81$ and $E = 0.44$, respectively. The intensity ratio β of signal to pump beams can be adjusted by changing the transmittance intensity through an attenuator in a pump beam of Fig 1.

The experimental configuration for a cost function E = 0.44 is adopted to improve the correlation performance with relatively large gain $\Gamma = 19.6\ cm^{-1}$ and a long length $l = 0.42$ cm in the 45º-cut crystal. This hard-clipping characteristics is shown in a red solid line of Fig 6. The amplitude of the high-frequency component of the object using the 45º-cut crystal is enhanced more than using the 0º-cut crystal. The smaller the amplitude of the input signal beam is, the more the signal-beam amplitude is enhanced.

The nonlinear response shown by a dotted line in Fig 6 best exhibits the hard-clipping nonlinearity. However this interaction length $l = 0.55$ cm cannot be realized because the 45º-cut crystal size is small.

Figure 7 shows the experimental results of correlating the enhanced 50-yen stamp spectrum with the POF of a 50-yen mailing stamp, and the enhanced 80-yen stamp spectrum with the POF of a 50-yen stamp. In Fig 7, above part shows the cross-sectional correlation peaks, whereas the below part shows the three-dimensional plots of the correlation peaks. As a comparison, Fig 7 exhibits an intense autocorrelation between the enhanced spectrum A_S of a 50-yen stamp and the POF of a 50-yen stamp, and a weak cross-correlation between the enhanced 80-yen stamp spectrum and the POF of a 50-yen stamp using the two-wave mixing with a 45º-cut $BaTiO_3$ crystal.

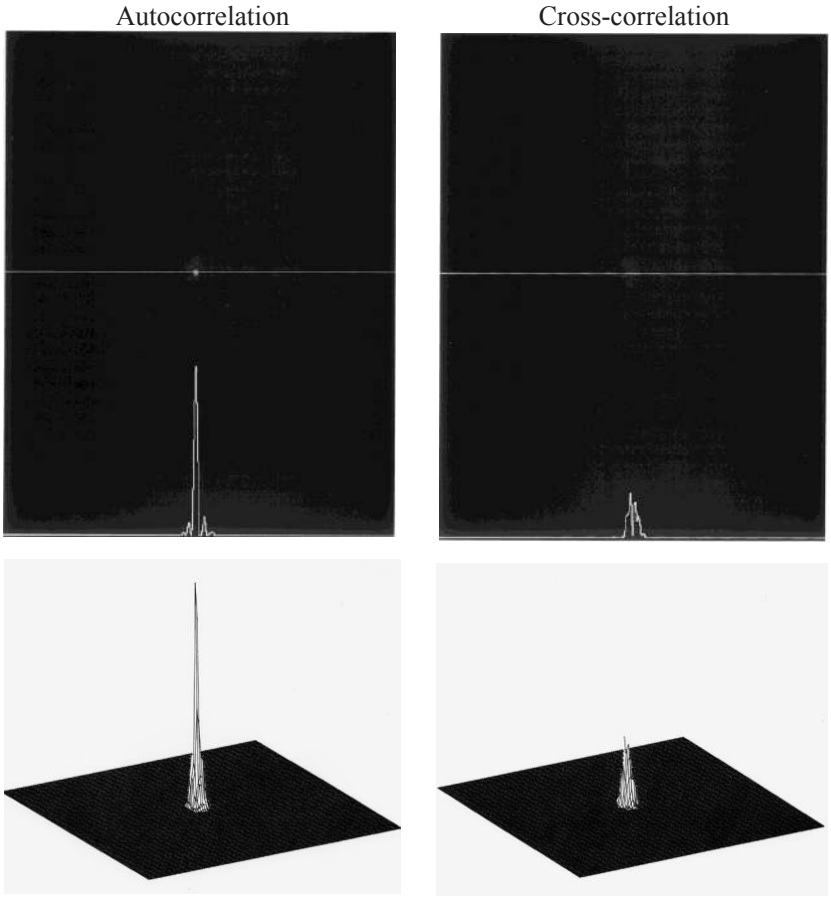

Fig 7. Experimental correlation signals obtained by a spectrum-enhanced correlator using a 45º-cut $BaTiO_3$ crystal; autocorrelation (left) and cross-correlation (right).

Discrimination capability (DC) is introduced to check the correlation performance. DC is defined as the quotient between the autocorrelation maximum minus cross-correlation maximum and the autocorrelation maximum. The 45º-cut $BaTiO_3$ crystal has a higher DC from DC= 0.75 to 0.85 than the 0º-cut crystal, and improves the correlation performance of identifying the similar objects as shown in Fig 5. An intensity difference between auto- and cross-correlations has increased in the correlator consisting of the spectrum-enhanced pre-processor with the high-gain coupling coefficient and the phase-only filter. In addition, a

correlator using only a phase-only filter has the lowest discrimination capability with DC=0.65 among the three types of correlators.

4 Conclusion

Spectrum-enhanced correlator by two-wave mixing in a photorefractive crystal has been constructed to improve the correlation performance by using a phase-only filter. The photorefractive gain has tailored that the small input signal containing high frequency components can be amplified. Two-wave mixing in a 45º-cut $BaTiO_3$ crystal is carried out between an object to be enhanced and a pump beam. Beam-propagation calculation inside a crystal shows the gaining process of the spectral amplitudes of an object by a two-wave mixing. The enhanced propagated spectra in high frequencies are numerically shown along a crystal depth. High discriminate correlation results are shown in the pattern-recognition experiments.

Prof. Asakura has rendered most excellent services in optical physics and technology and has navigated worldwide optical community with strong and kind leadership as a past *ICO* president. One of the authors (YI) greatly appreciates his continuous guidance and encouragement to my research activity. YI also greatly honors and appreciates his distinguished professional activities for the optical community

References

1. Francis T S Yu, Jutamulia S, Yin S, Introduction to Information Optics, (Academic Press, San Diego), 2001.
2. Javidi B, *Appl Opt*, 28(1989)2358-2367.
3. Horner J L, Gianino P D, *Appl Opt*, 23(1984)812-816.
4. Ishii Y, Takahashi T, Kobayashi M, *Opt Commun*, 132(1996)153-160.
5. Takahashi T, Ishii Y, *Appl Opt*, 36(1997)1073-1085.
6. Ersoy O K, Zeng M, *J Opt Soc Am A*, 6(1989)636-648.
7. Nomura T, Itoh K, Matsuoka K, Ichioka Y, *Opt Lett*, 15(1990) 810-811.
8. Uhrich C, Hesselink L, *Appl Opt*, 27(1988)4497-4503.
9. Solymar L, Webb D J, Grunnet-Jepsen A, The physics and applications of photorefractive materials, (Clarendon Press, Oxford), 1996, Chap. 10.
10. Khoury J, Cronin-Golomb M, Gianino P, Woods C, *J Opt Soc Am B*, 11(1994)2167-2174.
11. Pati G S, Tripathi R, Singh K, *Opt Commun,*151(1998)268-272.
12. Tripathi R, Pati G S, Singh K, *Opt Eng*, 37(1998)2148; doi.org/10.1117/1.601718
13. Koukourakis N, Abdelwahab T, Li M Y, Höpfner H, Lai Y W, Darakis E, Brenner C, Gerhardt N, Hofmann M, *Opt Express*, 19 (2011)22004-22023.
14. Ishii Y, Takahashi T, *Proc SPIE*, 5206(2003)90; doi.org/10.1117/12.508124
15. Pepper D M, *Appl Phys Lett*, 49(1998)1001-1003
16. Ford J E, Fainman Y, Lee S H, *Appl Opt,* 28(1989)4808-4815.
17. Yeh P, Introduction to Photorefractive Nonlinear Optics, Sect. 4.1.1, (Wiley, New York), 1993, .
18. Rigler A K, Pegis R J, Optimization methods in optics in The computer in optical research, Topics in applied physics, Volume 41, Frieden B R(Ed), (Springer, Berlin),1980.
19. Ahouzi E, Campos J, Chałasinska-Macukow K, Yzuel M J, *Opt. Commun*,110(1994)27-32.
20. Goodman J, *Introduction to Fourier optics,* (McGraw-Hill, New York, 2nd Ed.) 1996, p57.

[*Received:* 26.10.2018; *accepted*: 25.11.18]

Yukihiro Ishii

Yukihiro Ishii received Ph. D. degree from Hokkaido University in 1984. Since 1989, he had been a Professor at Electronics Department, University of Industrial Technology (Polytechnic Univ.), Japan. Since 2005, he had been a Professor at Department of Applied Physics, Tokyo University of Science (TUS), Tokyo, and since 2011 after retirement, he is been a Professor of part-time, TUS, giving lectures of physics and optical electronics, and a Riken visiting scientist. He has authored over 100 technical journal articles. His current interests include laser-diode interferometry, holography and nonlinearphotorefractive optics. He is Fellow of OSA, SPIE and JSAP.

Takeshi Takahashi

Takeshi Takahashi received his BS degree in applied physics from Tokyo University of Agriculture and Technology, Tokyo, in 1989, and his Ph. D. Degree from Saitama University in 2006. Since 1993, he had been Research Associate at University of Industrial Technology, Sagamihara, Japan, where since 2012 he has been Associate Professor at Polytechnic University, Tokyo. His current interests are digital holography and computational optics. He is a member of OSJ and JSAP.